Research Square

Preprints are preliminary reports that have not undergone peer review.
They should not be considered conclusive, used to inform clinical practice,
or referenced by the media as validated information.

Attitude Estimation using Redundant Gyros

Andrea Rigato

andrea.rigato@utexas.edu

The University of Texas at Austin

Renato Zanetti

The University of Texas at Austin

Research Article

Keywords: attitude estimation, MEKF, gyros

Posted Date: November 13th, 2026

DOI: https://doi.org/10.21203/rs.3.rs-11322705/v1

License: This work is licensed under a Creative Commons Attribution 4.0 International License.
Read Full License

Additional Declarations: No competing interests reported.

Attitude Estimation using Redundant Gyros

Andrea Rigato[1*] and Renato Zanetti[1]

[1*]Department of Aerospace Engineering and Engineering Mechanics, The University of Texas at Austin, Austin, 78712, TX, United States.

*Corresponding author(s). E-mail(s): andrea.rigato@utexas.edu;
Contributing authors: renato@utexas.edu;

Abstract

Precise attitude estimation is a critical requirement for most space missions to ensure accurate spacecraft orientation and control. Sensor redundancy is essential for fault detection and isolation (FDI), improving reliability and robustness. Current onboard attitude determination systems typically rely on a single gyro to propagate the state and a star tracker (or other aiding source) to update it; additional gyros are used solely for FDI. This approach, however, underutilizes available measurements, potentially limiting estimation accuracy. This work proposes a novel attitude estimation framework that incorporates measurements from all available gyros, improving estimation precision while preserving the observability of individual gyro biases. The proposed method averages measurements from gyros with similar noise characteristics for state propagation, while the measurement difference is leveraged in a subsequent update step. Optimality of the method is analytically demonstrated for a planar rotation scenario, and its performance is assessed through numerical simulations in the three-dimensional case.

Keywords: attitude estimation, MEKF, gyros

1 Introduction

Redundancy is a critical requirement in space missions, particularly in sensor systems, where it ensures the reliable detection and isolation of faults. In spacecraft attitude estimation, multiple three-axis gyros are commonly employed to enhance reliability and robustness. For instance, NASA's Orion spacecraft [1] and the Space Shuttle [2] were both equipped with three inertial measurement units (IMUs). An IMU normally

contains a three-axis gyro and a three-axis accelerometer. In this work, we focus on attitude estimation and therefore consider only redundant gyros.

Gyroscopic measurements play a fundamental role in the so-called dynamic model replacement approach [3]. In model replacement, gyros propagate the spacecraft's attitude dynamics, replacing a torque model, which is difficult to characterize accurately. To counteract gyro drift and measurement errors, other sensors, like star trackers, are fused with gyro data, preventing the state estimate from diverging over time.

The typical approach for spacecraft attitude estimation predominantly relies on a single gyro measurement for state propagation, while the remaining gyros are used exclusively for FDI. Both Orion [1] and the Space Shuttle [4] utilized three IMUs to enable a center-select algorithm for efficient fault detection and isolation. This algorithm operates by selecting a reference value, typically the median, from a set of redundant sensors. Any measurement that deviates beyond a predefined threshold is classified as faulty and subsequently discarded. Additionally, Orion's fault detection and isolation system incorporates a parity algorithm [5] to determine the most reliable IMU when all three are operational.

Recent research [6, 7] has demonstrated that averaging measurements from multiple IMUs can yield a more precise estimate. In particular, de Alteriis et al. [6] showed that by combining data from six low-grade gyros, it is possible to achieve a level of accuracy comparable to that of a tactical-grade gyro. While this approach enhances measurement precision, it can overlook the observability of individual gyro biases. Accurate estimation of these biases is essential for detecting and isolating faults, as unobservable biases can degrade system performance and allow sensor failures to go undetected.

Patel et al. [8] compared various methods for fusing measurements from multiple IMUs. Their proposed approaches emphasize accelerometer and magnetometer readings, treating them as direct measurements, while the handling of gyro data is not discussed in detail. Similarly, Beaudoin et al. [9] explored three different strategies for handling multiple IMUs in a space launch vehicle. In their formulation, angular velocity is included as a state variable with uncertain dynamics and is estimated as part of the filtering process, rather than being obtained through direct integration of gyro measurements. Consequently, gyro measurements are treated as direct observations of the state instead of inputs used to propagate it.

More recently, Marcus et al. [10] proposed a method in which one gyro is used to propagate the attitude state, while the remaining gyros are utilized for the state update. This configuration preserves the full observability of each individual gyro bias. Additionally, the paper introduces the concept of a synthetic gyro, formed by simply averaging the measurements from all available gyros. This alternative approach is shown to numerically yield the same attitude estimate as the former; however, it does not retain observability of the individual gyro biases. Moreover, it assumes that all gyros have identical noise characteristics.

This work considers the problem of attitude estimation using redundant gyros and presents two main contributions.[1] The first contribution is a theoretical result

[1] This work extends the preliminary results presented at the 2025 AAS/AIAA Astrodynamics Specialist Conference [11]. While the previous study focused on planar rotation and provided an in-depth treatment of the two-dimensional case, the present work generalizes the algorithm to handle three-dimensional rotations.

establishing that, in the planar rotation case, propagating the attitude using an averaged angular velocity yields the same attitude estimate as propagating the state with a single gyro measurement and incorporating the remaining measurement in the update step. The second contribution is the development of a new attitude estimation framework that exploits all available gyro measurements while preserving individual bias observability. The method builds upon the concept of propagating the state using an averaged angular velocity introduced by Marcus et al. [10], but introduces a novel update strategy: the difference between individual angular velocity measurements are also used as observations to maintain bias observability. The statistical correlation between the averaged measurement used in propagation and the differential measurement used in the update is explicitly analyzed. In the planar rotation case, this approach is shown to be mathematically equivalent to using different gyro measurements in the propagation and update steps. For general three-dimensional rotations, where exact equivalence is lost due to linearization, Monte Carlo simulations demonstrate that the proposed method achieves numerically equivalent performance.

The remainder of this paper is organized as follows. Section 2 demonstrates that propagating the attitude using the averaged angular velocity or using individual gyro measurements in the propagation and update steps leads to the same attitude estimate for a planar rotation scenario with bias-free gyros. Section 3 extends this result to the case of biased angular measurements and introduces the proposed filter, which preserves individual bias observability. Section 4 then generalizes the proposed filter to three-axis rotations, developing a modified multiplicative extended Kalman filter (MEKF). Finally, section 5 presents the conclusions of this study.

2 Planar Rotation with Bias-Free Gyro Measurements

This section compares two different methodologies for estimating a planar rotation using measurements from two bias-free gyros. Specifically, we want to estimate the angle $\theta(t)$ whose continuous time dynamics are

$$\dot{\theta}(t) = \omega(t), \tag{1}$$

where $\omega(t)$ is the angular velocity. Assuming a slowly varying angular velocity and a sufficiently high sampling rate, the discrete-time dynamics can be approximated using a backward Euler step [12]:

$$\theta_k = \theta_{k-1} + \omega_k \Delta t, \tag{2}$$

where $\Delta t = t_k - t_{k-1}$, θ_k is the angle at time k, and ω_k is the angular velocity at time k. At time k, measurements from two gyros are available. Throughout this paper, the superscript (i) denotes a quantity associated with the *i-th* gyro and a tilde $\widetilde{(.)}$ is used to denote that $(.)$ is a measured quantity, and a hat $\hat{(.)}$ is used to denote an estimate of $(.)$. The measurement model is

$$\widetilde{\omega}_k^{(i)} = \frac{1}{\Delta t}\left(\theta_k - \theta_{k-1}\right) + \nu_k^{(i)}, \quad i = 1, 2, \tag{3}$$

where $\nu_k^{(i)} \sim \mathcal{N}(0, \sigma_{(i)}^2)$ is a Gaussian white sequence. Furthermore, the two gyros are assumed to be uncorrelated, hence

$$\mathbb{E}[\nu_k^{(i)} \nu_k^{(j)}] = \sigma_{(i)}^2 \delta_{ij}, \tag{4}$$

where the noise standard deviation $\sigma_{(i)}$ is associated with the angular random walk (ARW) and the sampling rate Δt through the relation

$$\sigma_{(i)} = \frac{\mathrm{ARW}^{(i)}}{\sqrt{\Delta t}}. \tag{5}$$

The goal is estimating the angle θ_k, given the posterior distribution $\theta_{k-1} \sim \mathcal{N}(\hat{\theta}_{k-1}, P_{k-1})$ at time $k-1$ and measurements $\widetilde{\omega}_k^{(1)}$, $\widetilde{\omega}_k^{(2)}$ at time k. Examining eqs. (2) and (3), it is possible to infer that the angular velocity provided by the gyros can either be used as an input to propagate the state estimate from time $k-1$ to k or as a measurement to update the estimate at time k. This section analyzes this duality and explores the differences, if any, between using the gyro data as an input versus as a measurement.

The dynamics reported in eq. (2) and the measurement function in eq. (3) are linear with respect to the state, and the initial condition is assumed to be Gaussian-distributed. For linear Gaussian systems, the Kalman Filter [13] is the optimal estimator in both the maximum a posteriori (MAP) sense and the minimum mean square error (MMSE) sense [14]. Therefore, we use the Kalman filter framework to compare the proposed methodologies.

2.1 Time and Measurement Updates Using Distinct Gyros

At time k, we have two angular velocity measurements. Since angular velocity can be used either as an input to the dynamics or as a measurement, a natural approach is to use one angular velocity measurement to propagate the estimate of the angle and the other to update it. Specifically, we use the measurement $\widetilde{\omega}_k^{(1)}$ from gyro 1 as an input and the measurement $\widetilde{\omega}_k^{(2)}$ from gyro 2 as an observation. The final estimate remains unchanged if the roles of the two gyros are reversed.

2.1.1 Time update

A generic linear system, subject to uncertain input $\boldsymbol{u}_{k-1}$ and no process noise, can be described as:

$$\boldsymbol{x}_k = \boldsymbol{\Phi} \boldsymbol{x}_{k-1} + \boldsymbol{B} \boldsymbol{u}_{k-1}, \tag{6}$$

where $\boldsymbol{\Phi}$ is the state transition matrix mapping the state from time $k-1$ to time k, and $\boldsymbol{B}$ is the control matrix. Given an initial Gaussian distribution $\boldsymbol{x}_{k-1} \sim \mathcal{N}(\hat{\boldsymbol{x}}_{k-1}, \boldsymbol{P}_{k-1})$, and a Gaussian distributed input $\boldsymbol{u}_{k-1} \sim \mathcal{N}(\hat{\boldsymbol{u}}_{k-1}, \boldsymbol{U}_{k-1})$ the distribution remains Gaussian throughout the process, i.e. $\boldsymbol{x}_k \sim \mathcal{N}(\bar{\boldsymbol{x}}_k, \bar{\boldsymbol{P}}_k)$, where:

$$\bar{\boldsymbol{x}}_k = \boldsymbol{\Phi} \hat{\boldsymbol{x}}_{k-1} + \boldsymbol{B} \hat{\boldsymbol{u}}_{k-1}, \tag{7}$$

$$\bar{\boldsymbol{P}}_k = \boldsymbol{\Phi}\boldsymbol{P}_{k-1}\boldsymbol{\Phi}^T + \boldsymbol{B}\boldsymbol{U}_{k-1}\boldsymbol{B}^T. \tag{8}$$

For a planar rotation, when the input is the angular velocity measured by gyro 1, we get

$$\hat{\boldsymbol{u}}_{k-1} = \widetilde{\omega}_k^{(1)}, \quad \boldsymbol{\Phi} = 1, \quad \boldsymbol{B} = \Delta t, \quad \boldsymbol{U}_{k-1} = \sigma^2_{(1)}, \tag{9}$$

and, consequently, the propagated distribution at time k is $\theta_k \sim \mathcal{N}(\bar{\theta}_k, \bar{P}_k)$ where:

$$\bar{\theta}_k = \hat{\theta}_{k-1} + \widetilde{\omega}_k^{(1)}\Delta t, \tag{10}$$

$$\bar{P}_k = P_{k-1} + \Delta t^2 \sigma^2_{(1)}. \tag{11}$$

2.1.2 Measurement update

To incorporate the information from gyro 2, it is necessary to modify the Kalman update [13] to account for the fact that the measurement $\boldsymbol{z}_k$ is a linear function of the state at both time k and $k-1$:

$$\boldsymbol{z}_k = \boldsymbol{H}\boldsymbol{x}_k + \boldsymbol{J}\boldsymbol{x}_{k-1} + \boldsymbol{v}_k, \tag{12}$$

where $\boldsymbol{v}_k \sim \mathcal{N}(\boldsymbol{0}, \boldsymbol{R})$. The dependence of the measurement on the state at time $k-1$ introduces a correlation between the state error and the measurement error, which must be addressed by reformulating the Kalman update. The delayed state Kalman update proposed by Brown and Hwang [15], which is followed in this paper, derives a new Kalman gain as:

$$\begin{aligned}\boldsymbol{K}_k = &\left(\bar{\boldsymbol{P}}_k\boldsymbol{H}^T + \boldsymbol{\Phi}\boldsymbol{P}_{k-1}\boldsymbol{J}^T\right)\cdot \\ &\left(\boldsymbol{H}\bar{\boldsymbol{P}}_k\boldsymbol{H}^T + \boldsymbol{R} + \boldsymbol{J}\boldsymbol{P}_{k-1}\boldsymbol{\Phi}^T\boldsymbol{H}^T + \boldsymbol{H}\boldsymbol{\Phi}\boldsymbol{P}_{k-1}\boldsymbol{J}^T + \boldsymbol{J}\boldsymbol{P}_{k-1}\boldsymbol{J}^T\right)^{-1}.\end{aligned} \tag{13}$$

The update step becomes

$$\hat{\boldsymbol{x}}_k = \bar{\boldsymbol{x}}_k + \boldsymbol{K}_k\left(\boldsymbol{z}_k - \boldsymbol{H}\bar{\boldsymbol{x}}_k - \boldsymbol{J}\bar{\boldsymbol{x}}_{k-1}\right), \tag{14}$$

$$\boldsymbol{P}_k = \bar{\boldsymbol{P}}_k - \boldsymbol{K}_k\boldsymbol{L}_k\boldsymbol{K}_k^T, \tag{15}$$

where:

$$\boldsymbol{L}_k = \boldsymbol{H}\bar{\boldsymbol{P}}_k\boldsymbol{H}^T + \boldsymbol{R} + \boldsymbol{J}\boldsymbol{P}_{k-1}\boldsymbol{\Phi}^T\boldsymbol{H}^T + \boldsymbol{H}\boldsymbol{\Phi}\boldsymbol{P}_{k-1}\boldsymbol{J}^T + \boldsymbol{J}\boldsymbol{P}_{k-1}\boldsymbol{J}^T. \tag{16}$$

In the case considered, we use the angular velocity of gyro 2 as a measurement, and therefore

$$\boldsymbol{z}_k = \widetilde{\omega}_k^{(2)}, \quad \boldsymbol{H} = \frac{1}{\Delta t}, \quad \boldsymbol{J} = -\frac{1}{\Delta t}, \quad \boldsymbol{R} = \sigma^2_{(2)}. \tag{17}$$

It follows that

$$\boldsymbol{K}_k = \Delta t \frac{\sigma^2_{(1)}}{\sigma^2_{(1)} + \sigma^2_{(2)}}, \tag{18}$$

$$\boldsymbol{L}_k = \sigma^2_{(1)} + \sigma^2_{(2)}, \tag{19}$$

and the update step is given by

$$\hat{\theta}_k = \bar{\theta}_k + \Delta t \frac{\sigma^2_{(1)}}{\sigma^2_{(1)} + \sigma^2_{(2)}} \left(\widetilde{\omega}^{(2)}_k - \widetilde{\omega}^{(1)}_k \right), \tag{20}$$

$$P_k = \bar{P}_k - \Delta t^2 \frac{\sigma^4_{(1)}}{\sigma^2_{(1)} + \sigma^2_{(2)}}. \tag{21}$$

Substituting eqs. (10) and (11), into eqs. (20) and (21), the posterior distribution at time k given a previous distribution $\theta_{k-1} \sim \mathcal{N}(\hat{\theta}_{k-1}, P_{k-1})$ and measurements $\omega^{(1)}_k$, $\omega^{(2)}_k$, is $\theta_k \sim \mathcal{N}(\hat{\theta}_k, P_k)$, where

$$\hat{\theta}_k = \hat{\theta}_{k-1} + \Delta t \frac{\sigma^2_{(2)} \widetilde{\omega}^{(1)}_k + \sigma^2_{(1)} \widetilde{\omega}^{(2)}_k}{\sigma^2_{(1)} + \sigma^2_{(2)}}, \tag{22}$$

$$\hat{P}_k = \hat{P}_{k-1} + \Delta t^2 \frac{\sigma^2_{(1)} \sigma^2_{(2)}}{\sigma^2_{(1)} + \sigma^2_{(2)}}. \tag{23}$$

2.2 Time Update via Gyro Measurement Averaging

The previous section proposed an optimal method to propagate and update the estimate of the angle using two uncorrelated gyro measurements. This section demonstrates that averaging the gyro measurements leads to the same outcome.

Consider the weighted average angular rate:

$$\widetilde{\omega}^{(*)}_k = \frac{\sum_i \frac{1}{\sigma^2_{(i)}} \widetilde{\omega}^{(i)}_k}{\sum_i \frac{1}{\sigma^2_{(i)}}} = \frac{\sigma^2_{(2)} \widetilde{\omega}^{(1)}_k + \sigma^2_{(1)} \widetilde{\omega}^{(2)}_k}{\sigma^2_{(1)} + \sigma^2_{(2)}}. \tag{24}$$

It is trivial to prove that

$$\widetilde{\omega}^{(*)}_k \sim \mathcal{N}\left(\omega_k, \frac{\sigma^2_{(1)} \sigma^2_{(2)}}{\sigma^2_{(1)} + \sigma^2_{(2)}} \right), \tag{25}$$

where ω_k is the true angular velocity. The angle θ can be propagated from time $k-1$ to time k using the averaged angular velocity $\widetilde{\omega}^{(*)}_k$ as input in eqs. (7) and (8). The state distribution at time k is $\theta_k \sim \mathcal{N}(\hat{\theta}_k, P_k)$ where:

$$\hat{\theta}_k = \hat{\theta}_{k-1} + \Delta t \frac{\sigma^2_{(2)} \widetilde{\omega}^{(1)}_k + \sigma^2_{(1)} \widetilde{\omega}^{(2)}_k}{\sigma^2_{(1)} + \sigma^2_{(2)}}, \tag{26}$$

$$\hat{P}_k = \hat{P}_{k-1} + \Delta t^2 \frac{\sigma_{(1)}^2 \sigma_{(2)}^2}{\sigma_{(1)}^2 + \sigma_{(2)}^2}. \tag{27}$$

Comparing eqs. (22) and (23) with eqs. (26) and (27) demonstrates that propagating the angle θ using the weighted angular rate yields the same optimal estimate as propagating with one gyro measurement and updating with the other.

For the interested reader, a detailed discussion on the fusion of angular velocity models with gyro measurements, as well as the optimal averaging of correlated gyros, is provided in the appendix A.

3 Planar Rotation with Biased Gyro Measurements

The previous section showed how to use measurements coming from bias-free gyros to propagate the angle in an optimal way. However, to apply this approach to practical applications, biases must be incorporated into the measurement model for the gyros. This section introduces a method for averaging measurements from biased gyros under specific assumptions.

Consider measurements coming from two uncorrelated gyros

$$\widetilde{\omega}_k^{(i)} = \frac{1}{\Delta t}\left(\theta_k - \theta_{k-1}\right) + b_k^{(i)} + \nu_k^{(i)}, \quad i = 1, 2, \tag{28}$$

where $b_k^{(i)}$ is the bias of the *i-th* gyro at time k. The bias drifts over time due to the bias instability. A mathematical model widely used to describe the evolution in time of the bias is given by [3]

$$\dot{b}^{(i)}(t) = \eta_b^{(i)}(t), \tag{29}$$

where $\eta_b^{(i)}(t)$ is a zero-mean Gaussian white-noise process. Under the assumption of a fast enough sampling rate, eq. (29) can be discretized considering $\eta_b^{(i)}(t)$ constant in the interval $k-1$ to k. It follows

$$b_k^{(i)} = b_{k-1}^{(i)} + \nu_k^{(i),b} \tag{30}$$

where $\nu_k^{(i),b}$ is a zero-mean Gaussian random sequence, i.e. $\nu_k^{(i),b} \sim \mathcal{N}(0, \sigma_{(i),b}^2)$. The estimated state is now

$$\boldsymbol{x}_k = \begin{bmatrix} \theta_k \\ b_k^{(1)} \\ b_k^{(2)} \end{bmatrix}. \tag{31}$$

The problem involves estimating the angle θ_k and the biases $b_k^{(1)}$, $b_k^{(2)}$, given the measurements $\widetilde{\omega}_k^{(1)}$ and $\widetilde{\omega}_k^{(2)}$, as well as the distribution of the state at the previous time $\boldsymbol{x}_{k-1} \sim \mathcal{N}(\hat{\boldsymbol{x}}_{k-1}, \boldsymbol{P}_{k-1})$.

In the remainder of the paper, we will adopt the simplification that the gyros are similar, meaning that their noise characteristics are in a constant ratio; i.e., the

following relationship holds

$$\frac{\sigma^2_{(1)}}{\sigma^2_{(2)}} = \frac{\sigma^2_{(1),b}}{\sigma^2_{(2),b}} = \frac{\operatorname{cov}\left(b_0^{(1)}\right)}{\operatorname{cov}\left(b_0^{(2)}\right)} = \rho. \tag{32}$$

In practical applications, redundant gyros are typically produced by the same manufacturer, resulting in identical noise specifications, i.e. $\rho = 1$. The following notation is used:

$$\sigma^2 = \sigma^2_{(2)} = \frac{\sigma^2_{(1)}}{\rho}, \quad \sigma^2_b = \sigma^2_{(2),b} = \frac{\sigma^2_{(1),b}}{\rho}. \tag{33}$$

3.1 Time and Measurement Updates Using Distinct Gyros

Similarly to what was done in the section 2.1, it is possible to use the measurement coming from gyro 1 as input to propagate the state, and the measurement coming from gyro 2 to perform the measurement update.

3.1.1 Time Update

For a linear system subjected to an uncertain input $\boldsymbol{u}_{k-1} \sim \mathcal{N}(\hat{\boldsymbol{u}}_{k-1}, \boldsymbol{U}_{k-1})$ and process noise $\boldsymbol{v}_{k-1} \sim \mathcal{N}(\boldsymbol{0}, \boldsymbol{Q}_{k-1})$, the dynamics are:

$$\bar{\boldsymbol{x}}_k = \boldsymbol{\Phi}\hat{\boldsymbol{x}}_{k-1} + \boldsymbol{B}\hat{\boldsymbol{u}}_{k-1}, \tag{34}$$

$$\bar{\boldsymbol{P}}_k = \boldsymbol{\Phi}\boldsymbol{P}_{k-1}\boldsymbol{\Phi}^T + \boldsymbol{B}\boldsymbol{U}_{k-1}\boldsymbol{B}^T + \boldsymbol{\Gamma}\boldsymbol{Q}_{k-1}\boldsymbol{\Gamma}^T, \tag{35}$$

where $\boldsymbol{\Gamma}$ is the process noise transition matrix. For a planar rotation with biased angular velocity measurements, it follows that:

$$\begin{gathered}\hat{\boldsymbol{u}}_{k-1} = \widetilde{\omega}^{(1)}_k, \quad \boldsymbol{\Phi} = \begin{bmatrix} 1 & -\Delta t & 0 \\ 0 & 1 & 0 \\ 0 & 0 & 1 \end{bmatrix}, \quad \boldsymbol{B} = \begin{bmatrix} \Delta t \\ 0 \\ 0 \end{bmatrix}, \\ \boldsymbol{\Gamma} = \begin{bmatrix} -\Delta t & 0 \\ 1 & 0 \\ 0 & 1 \end{bmatrix}, \quad \boldsymbol{U}_{k-1} = \rho\sigma^2, \quad \boldsymbol{Q}_{k-1} = \begin{bmatrix} \rho\sigma^2_b & 0 \\ 0 & \sigma^2_b \end{bmatrix}.\end{gathered} \tag{36}$$

3.1.2 Measurement Update

To perform the measurement update using the angular velocity coming from gyro 2, the modified Kalman update described in eqs. (12) to (16) is used. In the case considered, it is evident that:

$$\boldsymbol{H} = \begin{bmatrix} \frac{1}{\Delta t} & 0 & 1 \end{bmatrix}, \quad \boldsymbol{J} = \begin{bmatrix} -\frac{1}{\Delta t} & 0 & 0 \end{bmatrix}, \quad \boldsymbol{R} = \sigma^2. \tag{37}$$

Considering an initial distribution $\boldsymbol{x}_{k-1} \sim \mathcal{N}(\hat{\boldsymbol{x}}_{k-1}, \boldsymbol{P}_{k-1})$, where

$$\hat{\boldsymbol{x}}_{k-1} = \begin{bmatrix} \hat{\theta}_{k-1} \\ \hat{b}^{(1)}_{k-1} \\ \hat{b}^{(2)}_{k-1} \end{bmatrix}, \quad \boldsymbol{P}_{k-1} = \begin{bmatrix} P_{\theta\theta} & 0 & 0 \\ 0 & \rho P_{bb} & 0 \\ 0 & 0 & P_{bb} \end{bmatrix} \tag{38}$$

upon propagating the state using $\widetilde{\omega}^{(1)}_k$ and updating it using $\widetilde{\omega}^{(2)}_k$, the estimate at time k is given by:

$$\hat{\boldsymbol{x}}_k = \begin{bmatrix} \hat{\theta}_k \\ \hat{b}^{(1)}_k \\ \hat{b}^{(2)}_k \end{bmatrix} = \begin{bmatrix} \hat{\theta}_{k-1} + \Delta t \dfrac{\left(\widetilde{\omega}^{(1)}_k - b^{(1)}_{k-1}\right) + \rho\left(\widetilde{\omega}^{(2)}_k - b^{(2)}_{k-1}\right)}{1+\rho} \\ \hat{b}^{(1)}_{k-1} - \dfrac{\rho\left(P_{bb} + \sigma_b^2\right)\left(\widetilde{\omega}^{(2)}_k - b^{(2)}_{k-1} - \widetilde{\omega}^{(1)}_k + b^{(1)}_{k-1}\right)}{\mathrm{A}} \\ \hat{b}^{(2)}_{k-1} + \dfrac{\left(P_{bb} + \sigma_b^2\right)\left(\widetilde{\omega}^{(2)}_k - b^{(2)}_{k-1} - \widetilde{\omega}^{(1)}_k + b^{(1)}_{k-1}\right)}{\mathrm{A}} \end{bmatrix}, \tag{39}$$

$$\boldsymbol{P}_k = \begin{bmatrix} P_{\theta\theta} + \dfrac{\Delta t^2 P_{bb}\rho + \Delta t^2 \rho\sigma^2 + \Delta t^2 \rho\sigma_b^2}{\rho+1} & -\dfrac{\Delta t\,\mathrm{B}}{\rho+1} & -\dfrac{\Delta t\,\mathrm{B}}{\rho+1} \\ -\dfrac{\Delta t\,\mathrm{B}}{\rho+1} & \mathrm{B} - \dfrac{\mathrm{B}^2}{\mathrm{A}} & \dfrac{\mathrm{B}^2}{\rho\mathrm{A}} \\ -\dfrac{\Delta t\,\mathrm{B}}{\rho+1} & \dfrac{\mathrm{B}^2}{\rho\mathrm{A}} & P_{bb} + \sigma_b^2 - \dfrac{\left(P_{bb} + \sigma_b^2\right)^2}{\mathrm{A}} \end{bmatrix}, \tag{40}$$

where

$$\mathrm{A} = (\rho+1)\left(P_{bb} + \sigma^2 + \sigma_b^2\right), \tag{41}$$

$$\mathrm{B} = \rho\left(P_{bb} + \sigma_b^2\right). \tag{42}$$

The covariance matrix $\boldsymbol{P}_k$ associated with this estimate is not a sparse matrix, meaning that even if the state θ, $b^{(1)}$, and $b^{(2)}$ were initially uncorrelated, after the first update step they become correlated.

3.1.3 Transformation of variables

We propose a linear transformation of both the state and the input. This approach serves as the foundation for the new method introduced in the next section, where information from the two gyros are fused without relying on the delayed state update.

It is possible to introduce an average bias $b^{(*)}_k$ as

$$b^{(*)}_k = \frac{b^{(1)}_k + \rho\, b^{(2)}_k}{1+\rho}, \tag{43}$$

and a difference bias Δb_k as

$$\Delta b_k = b^{(1)}_k - b^{(2)}_k. \tag{44}$$

After this linear transformation, the state to be estimated becomes

$$\begin{bmatrix} \theta_k \\ b_k^{(1)} \\ b_k^{(2)} \end{bmatrix} \quad \Longrightarrow \quad \begin{bmatrix} \theta_k \\ b_k^{(*)} = \dfrac{b_k^{(1)} + \rho\, b_k^{(2)}}{1+\rho} \\ \Delta b_k = b_k^{(1)} - b_k^{(2)} \end{bmatrix}. \tag{45}$$

Similarly, it is possible to transform the measurements coming from the two gyros. We introduce an average angular velocity measurement $\widetilde{\omega}_k^{(*)}$ as

$$\widetilde{\omega}_k^{(*)} = \frac{\widetilde{\omega}_k^{(1)} + \rho\, \widetilde{\omega}_k^{(2)}}{1+\rho}, \tag{46}$$

and a difference angular velocity measurement $\Delta\widetilde{\omega}_k$ as

$$\Delta\widetilde{\omega}_k = \widetilde{\omega}_k^{(1)} - \widetilde{\omega}_k^{(2)}. \tag{47}$$

After applying these transformations to the state and input, the estimated state given by eqs. (39) and (40) becomes:

$$\hat{\boldsymbol{x}}_k = \begin{bmatrix} \hat{\theta}_k \\ \hat{b}_k^{(*)} \\ \Delta\hat{b}_k \end{bmatrix} = \begin{bmatrix} \hat{\theta}_{k-1} + \Delta t \left(\widetilde{\omega}_k^{(*)} - b_{k-1}^{(*)} \right) \\ \hat{b}_{k-1}^{(*)} \\ \dfrac{\sigma^2 \Delta\hat{b}_{k-1} + \left(P_{bb} + \sigma_b^2\right) \Delta\widetilde{\omega}_k}{\left(P_{bb} + \sigma^2 + \sigma_b^2\right)} \end{bmatrix}, \tag{48}$$

$$\boldsymbol{P}_k = \begin{bmatrix} P_{\theta\theta} + \Delta t^2 \dfrac{P_{bb}\rho + \rho\sigma^2 + \rho\sigma_b^2}{\rho+1} & -\dfrac{\Delta t \rho \left(P_{bb} + \sigma_b^2\right)}{\rho+1} & 0 \\ -\dfrac{\Delta t \rho \left(P_{bb} + \sigma_b^2\right)}{\rho+1} & \dfrac{\rho \left(P_{bb} + \sigma_b^2\right)}{\rho+1} & 0 \\ 0 & 0 & \dfrac{\sigma \left(P_{bb} + \sigma_b^2\right)(\rho+1)}{P_{bb} + \sigma^2 + \sigma_b^2} \end{bmatrix}. \tag{49}$$

Comparing eqs. (39) and (40) with eqs. (48) and (49) it is evident that these transformations maintain the same attitude propagation by using only the average angular rate and the average bias. Furthermore, the expected value of the average bias remains constant, while its covariance increases over time. The difference in biases depends solely on the difference in angular rates and is uncorrelated from both the average bias and the attitude.

3.2 Time Update via Gyro Measurement Averaging

In the previous section, we demonstrated that it is possible to propagate the attitude using only the average gyro measurement and the average bias. Building on this result,

in this section, we develop a new approach to estimate the angular rotation and the gyro biases without requiring the delayed state Kalman update.

3.2.1 Time Update

First, reconsider the linear transformation of the state described by eqs. (43) and (44). The following dynamics for the biases hold:

$$b_k^{(*)} = b_{k-1}^{(*)} + \nu_k^{(*),b}, \tag{50}$$

$$\Delta b_k = \Delta b_{k-1} + \nu_k^{\Delta b}, \tag{51}$$

where $\nu_k^{(*),b} \sim \mathcal{N}\left(0, \frac{\rho}{1+\rho}\sigma_b^2\right)$ and $\nu_k^{\Delta b} \sim \mathcal{N}\left(0, (1+\rho)\,\sigma_b^2\right)$. Furthermore, eq. (48) shows that the angle θ can be propagated as:

$$\theta_k = \theta_{k-1} + \Delta t \left(\widetilde{\omega}_k^{(*)} - b_k^{(*)}\right), \tag{52}$$

where $\widetilde{\omega}_k^{(*)} \sim \mathcal{N}\left(\omega_k, \frac{\rho}{1+\rho}\sigma^2\right)$.

Therefore, it is possible to perform a time update step starting from the estimate at time $k-1$. It is important to note that, due to the linear transformation of the state, the initial covariance matrix in this case is:

$$\boldsymbol{P}_{k-1} = \begin{bmatrix} P_{\theta\theta} & 0 & 0 \\ 0 & \frac{\rho}{1+\rho}P_{bb} & 0 \\ 0 & 0 & (1+\rho)\,P_{bb} \end{bmatrix}. \tag{53}$$

Utilizing eqs. (34) and (35), and using the average angular velocity to propagate the state

$$\begin{gathered} \hat{\boldsymbol{u}}_{k-1} = \widetilde{\omega}_k^{(*)}, \quad \boldsymbol{\Phi} = \begin{bmatrix} 1 & -\Delta t & 0 \\ 0 & 1 & 0 \\ 0 & 0 & 1 \end{bmatrix}, \quad \boldsymbol{B} = \begin{bmatrix} \Delta t \\ 0 \\ 0 \end{bmatrix}, \\ \boldsymbol{\Gamma} = \begin{bmatrix} -\Delta t & 0 \\ 1 & 0 \\ 0 & 1 \end{bmatrix}, \quad \boldsymbol{U}_{k-1} = \frac{\rho}{1+\rho}\sigma^2, \quad \boldsymbol{Q}_{k-1} = \begin{bmatrix} \frac{\rho}{1+\rho}\sigma_b^2 & 0 \\ 0 & (1+\rho)\,\sigma_b^2 \end{bmatrix}, \end{gathered} \tag{54}$$

the prior estimate at time k is:

$$\bar{\boldsymbol{x}}_k = \begin{bmatrix} \hat{\theta}_k \\ \hat{b}_k^{(*)} \\ \Delta\hat{b}_k \end{bmatrix} = \begin{bmatrix} \hat{\theta}_{k-1} + \Delta t \left(\widetilde{\omega}_k^{(*)} - b_{k-1}^{(*)}\right) \\ \hat{b}_{k-1}^{(*)} \\ \Delta\hat{b}_{k-1} \end{bmatrix}, \tag{55}$$

$$\bar{\boldsymbol{P}}_k = \begin{bmatrix} P_{\theta\theta} + \Delta t^2 \dfrac{P_{bb}\rho + \rho\sigma^2 + \rho\sigma_b^2}{\rho+1} & -\dfrac{\Delta t\rho\left(P_{bb}+\sigma_b^2\right)}{\rho+1} & 0 \\ -\dfrac{\Delta t\rho\left(P_{bb}+\sigma_b^2\right)}{\rho+1} & \dfrac{\rho\left(P_{bb}+\sigma_b^2\right)}{\rho+1} & 0 \\ 0 & 0 & \left(P_{bb}+\sigma_b^2\right)(\rho+1) \end{bmatrix}. \tag{56}$$

By comparing eqs. (48) and (49) with eqs. (55) and (56), it is clear that while the expected values and covariances of the angle θ and the average bias are identical between the two methods, the estimate of the difference in biases is not. This discrepancy arises because only a linear combination of the two inputs is used, neglecting information that could be obtained by considering each input individually.

3.2.2 Measurement Update

The method we propose involves updating the state using the difference in the angular velocities of the gyros, after propagating the state with the average angular rate. Equations (57) to (60) show that the difference in the angular velocities of the gyros directly corresponds to the difference in biases. Therefore, it is possible to perform a standard Kalman update since the measurement depends solely on the state at time k

$$\begin{aligned} \Delta\widetilde{\omega}_k &= \widetilde{\omega}_k^{(1)} - \widetilde{\omega}_k^{(2)} && (57)\\ &= \widetilde{\omega}_k + b_k^{(1)} + \nu^{(1)} - \widetilde{\omega}_k - b_k^{(2)} - \nu^{(2)} && (58)\\ &= b_k^{(1)} - b_k^{(2)} - \nu^{(2)} + \nu^{(1)} && (59)\\ &= \Delta b_k + \nu_k^{\Delta}, && (60) \end{aligned}$$

where $\nu_k^{\Delta} \sim \mathcal{N}\left(0, (1+\rho)\,\sigma^2\right)$.

Considering the measurement function:

$$\boldsymbol{z}_k = \boldsymbol{H}\boldsymbol{x}_k + \boldsymbol{v}_k, \tag{61}$$

where $\boldsymbol{v}_k \sim \mathcal{N}(\boldsymbol{0}, \boldsymbol{R})$ and

$$\boldsymbol{H} = \begin{bmatrix} 0 & 0 & 1 \end{bmatrix}, \quad \boldsymbol{R} = (1+\rho)\,\sigma^2 \tag{62}$$

and considering the Kalman update:

$$\begin{aligned} \boldsymbol{K}_k &= \left(\bar{\boldsymbol{P}}_k \boldsymbol{H}^T\right)\left(\boldsymbol{H}\bar{\boldsymbol{P}}_k\boldsymbol{H}^T + \boldsymbol{R}\right)^{-1}, && (63)\\ \hat{\boldsymbol{x}}_k &= \bar{\boldsymbol{x}}_k + \boldsymbol{K}_k\left(\boldsymbol{z}_k - \boldsymbol{H}\bar{\boldsymbol{x}}_k\right), && (64)\\ \boldsymbol{P}_k &= \bar{\boldsymbol{P}}_k - \boldsymbol{K}_k\boldsymbol{H}\bar{\boldsymbol{P}}_k. && (65) \end{aligned}$$

It follows that, after the update, the estimated state is:

$$\hat{\boldsymbol{x}}_k = \begin{bmatrix} \hat{\theta}_k \\ \hat{b}_k^{(*)} \\ \Delta\hat{b}_k \end{bmatrix} = \begin{bmatrix} \hat{\theta}_{k-1} + \Delta t \left(\widetilde{\omega}_k^{(*)} - b_{k-1}^{(*)} \right) \\ \hat{b}_{k-1}^{(*)} \\ \dfrac{\sigma^2 \Delta\hat{b}_{k-1} + \left(P_{bb} + \sigma_b^2 \right) \Delta\widetilde{\omega}_k}{\left(P_{bb} + \sigma^2 + \sigma_b^2 \right)} \end{bmatrix}, \tag{66}$$

$$\boldsymbol{P}_k = \begin{bmatrix} P_{\theta\theta} + \Delta t^2 \dfrac{P_{bb}\rho + \rho\sigma^2 + \rho\sigma_b^2}{\rho + 1} & -\dfrac{\Delta t \rho \left(P_{bb} + \sigma_b^2 \right)}{\rho + 1} & 0 \\ -\dfrac{\Delta t \rho \left(P_{bb} + \sigma_b^2 \right)}{\rho + 1} & \dfrac{\rho \left(P_{bb} + \sigma_b^2 \right)}{\rho + 1} & 0 \\ 0 & 0 & \dfrac{\sigma \left(P_{bb} + \sigma_b^2 \right) (\rho + 1)}{P_{bb} + \sigma^2 + \sigma_b^2} \end{bmatrix}. \tag{67}$$

By comparing eqs. (48) and (49) with eqs. (66) and (67), it is clear that the estimated state and covariance are the same. We have thus proved that propagating the state using the measurement from one gyro and updating the state with the measurement from the other gyro, while employing the delayed state update, is equivalent to propagating the state with the average measurement $\widetilde{\omega}^{(*)}$ and performing a standard Kalman update using the difference measurement $\Delta\widetilde{\omega}$.

Furthermore, we demonstrated that, through the linear transformation of the biases, the difference in biases Δb is uncorrelated from both the average bias $b^{(*)}$ and the angle θ. This implies that, for estimating the attitude θ_k in the MMSE or MAP sense (which coincide under the linear-Gaussian assumptions of the filter), only the propagation step with $\widetilde{\omega}^{(*)}$ is necessary; the subsequent update with the difference measurement provides no further information about θ_k and thus yields zero gain for the attitude estimate. The update step does, however, make the difference in biases observable and is therefore useful if the goal is to determine the individual gyro biases, for example for fault detection and isolation purposes. For the interested reader, a formal observability analysis of the system is presented in appendix B.

4 Three-Dimensional Rotation with Biased Gyro Measurements

This section extends the filter proposed in section 3.2 to three-dimensional rotations. First, section 4.1 briefly reviews the MEKF. Then, section 4.2 presents our novel filter applied to a spatial rotation scenario. Finally, section 4.3 conducts a Monte Carlo simulation to compare the proposed approach with the method presented by Marcus et al. [10].

4.1 Multiplicative Extended Kalman Filter

Spacecraft attitude estimation commonly relies on unit quaternions $\boldsymbol{q}$ to represent the rotation from an inertial reference frame to a body-fixed frame. Although quaternions

provide a singularity-free and compact parametrization of three-dimensional rotations, they possess one degree of redundancy: the unit-norm constraint given by $\|\boldsymbol{q}\| = 1$. Attitude composition via quaternion multiplication is not commutative and not the same as adding two quaternions.

To circumvent the non-additive nature of rotations and enable effective application of linear estimation techniques such as the extended Kalman filter (EKF), the MEKF is widely employed [16]. In the MEKF, the estimated attitude is represented by a reference quaternion $\hat{\boldsymbol{q}}$, while the state vector maintains only a three-dimensional error representation, typically a small rotation vector. The true attitude quaternion is then reconstructed multiplicatively as

$$\boldsymbol{q} = \delta\boldsymbol{q} \otimes \hat{\boldsymbol{q}}, \tag{68}$$

where the symbol $\otimes$ denotes the Shuster product [17], and $\delta\boldsymbol{q}$ denotes the small attitude error

$$\boldsymbol{\delta q} \approx \frac{1}{\sqrt{1 + \|\boldsymbol{\delta\alpha}/2\|^2}} \begin{bmatrix} \boldsymbol{\delta\alpha}/2 \\ 1 \end{bmatrix} \tag{69}$$

for small angles $\boldsymbol{\delta\alpha}$. This error-state formulation preserves the unit-norm constraint exactly and allows linearization of the measurement and process models around the identity error.

4.2 Time Update via Gyro Measurement Averaging

As for the planar case, we are considering the assumption of similar gyros, meaning the noise characteristics of the two gyros are in a constant ratio. In particular, considering the measurement model:

$$\widetilde{\boldsymbol{\omega}}_k^{(i)} = \boldsymbol{\omega}_k + \boldsymbol{b}_k^{(i)} + \boldsymbol{\nu}_k^{(i)}, \quad i = 1, 2, \tag{70}$$

where $\boldsymbol{\nu}_k^{(i)} \sim \mathcal{N}(\boldsymbol{0}, \sigma_{(i)}^2 \boldsymbol{I}_{3\times 3})$ and in which:

$$\boldsymbol{b}_k^{(i)} = \boldsymbol{b}_{k-1}^{(i)} + \boldsymbol{\nu}_k^{(i),b}, \tag{71}$$

where $\boldsymbol{\nu}_k^{(i),b} \sim \mathcal{N}(\boldsymbol{0}, \sigma_{(i),b}^2 \boldsymbol{I}_{3\times 3})$. We assume that, by denoting the noises of gyro 2 as:

$$\sigma_{(2)}^2 = \sigma^2, \quad \sigma_{(2),b}^2 = \sigma_b^2, \quad \operatorname{cov}\left(\boldsymbol{b}_0^{(2)}\right) = \boldsymbol{P}_{bb}, \tag{72}$$

the noises of gyro 1 are:

$$\sigma_{(1)}^2 = \rho\,\sigma^2, \quad \sigma_{(1),b}^2 = \rho\,\sigma_b^2, \quad \operatorname{cov}\left(\boldsymbol{b}_0^{(1)}\right) = \rho\,\boldsymbol{P}_{bb}, \tag{73}$$

where ρ is a positive scalar. Under these assumptions, the average angular velocity $\widetilde{\boldsymbol{\omega}}_k^{(*)}$, defined as

$$\widetilde{\boldsymbol{\omega}}_k^{(*)} = \frac{\widetilde{\boldsymbol{\omega}}_k^{(1)} + \rho\, \widetilde{\boldsymbol{\omega}}_k^{(2)}}{1+\rho}, \tag{74}$$

is used to propagate the state, while the difference in angular velocity $\Delta\widetilde{\boldsymbol{\omega}}_k$, defined as

$$\Delta\widetilde{\boldsymbol{\omega}}_k = \widetilde{\boldsymbol{\omega}}_k^{(1)} - \widetilde{\boldsymbol{\omega}}_k^{(2)}. \tag{75}$$

is used to update the state. It is straightforward to prove that

$$\widetilde{\boldsymbol{\omega}}_k^{(*)} \sim \mathcal{N}\left(\boldsymbol{\omega}_k, \frac{\rho}{1+\rho}\sigma^2 \boldsymbol{I}_{3\times 3}\right), \tag{76}$$

$$\Delta\widetilde{\boldsymbol{\omega}}_k \sim \mathcal{N}\left(\Delta\boldsymbol{b}_k, (1+\rho)\,\sigma^2 \boldsymbol{I}_{3\times 3}\right). \tag{77}$$

Consider the following linear transformation of the biases of gyro 1 and gyro 2:

$$\boldsymbol{b}_k^{(*)} = \frac{\boldsymbol{b}_k^{(1)} + \rho\, \boldsymbol{b}_k^{(2)}}{1+\rho}, \tag{78}$$

$$\Delta\boldsymbol{b}_k = \boldsymbol{b}_k^{(1)} - \boldsymbol{b}_k^{(2)}. \tag{79}$$

The state we want to estimate becomes

$$\begin{bmatrix} \boldsymbol{\delta\alpha}_k \\ \boldsymbol{b}_k^{(1)} \\ \boldsymbol{b}_k^{(2)} \end{bmatrix} \quad \Longrightarrow \quad \begin{bmatrix} \boldsymbol{\delta\alpha}_k \\ \boldsymbol{b}_k^{(*)} \\ \Delta\boldsymbol{b}_k \end{bmatrix}. \tag{80}$$

It follows that the dynamics of the transformed biases is described by

$$\boldsymbol{b}_k^{(*)} = \boldsymbol{b}_{k-1}^{(*)} + \boldsymbol{\nu}_k^{(*),b}, \tag{81}$$

$$\Delta\boldsymbol{b}_k = \Delta\boldsymbol{b}_{k-1} + \boldsymbol{\nu}_k^{\Delta b}, \tag{82}$$

where $\boldsymbol{\nu}_k^{(*),b} \sim \mathcal{N}\left(\boldsymbol{0}, \frac{\rho}{1+\rho}\sigma_b^2 \boldsymbol{I}_{3\times 3}\right)$ and $\boldsymbol{\nu}_k^{\Delta b} \sim \mathcal{N}\left(\boldsymbol{0}, (1+\rho)\,\sigma_b^2 \boldsymbol{I}_{3\times 3}\right)$.

4.2.1 Time Update

Considering an initial distribution $\boldsymbol{x}_{k-1} \sim \mathcal{N}(\hat{\boldsymbol{x}}_{k-1}, \boldsymbol{P}_{k-1})$, where

$$\hat{\boldsymbol{x}}_{k-1} = \begin{bmatrix} \boldsymbol{\delta}\hat{\boldsymbol{\alpha}}_{k-1} \\ \hat{\boldsymbol{b}}_{k-1}^{(*)} \\ \Delta\hat{\boldsymbol{b}}_{k-1} \end{bmatrix}, \quad \boldsymbol{P}_{k-1} = \begin{bmatrix} \boldsymbol{P}_{\alpha\alpha} & \boldsymbol{0}_{3\times 3} & \boldsymbol{0}_{3\times 3} \\ \boldsymbol{0}_{3\times 3} & \frac{\rho}{1+\rho}\boldsymbol{P}_{bb} & \boldsymbol{0}_{3\times 3} \\ \boldsymbol{0}_{3\times 3} & \boldsymbol{0}_{3\times 3} & (1+\rho)\,\boldsymbol{P}_{bb} \end{bmatrix}. \tag{83}$$

The evolution of the state $\boldsymbol{\delta\alpha}$ is described by [16]

$$\boldsymbol{\delta\dot{\alpha}}(t) = [-\hat{\boldsymbol{\omega}}(t)]^{\times}\,\boldsymbol{\delta\alpha}(t) + \boldsymbol{\delta\omega}(t), \tag{84}$$

where $[-\hat{\boldsymbol{\omega}}(t)]^{\times}$ is the cross-produce skew-symmetric matrix associated with the estimated angular velocity $\hat{\boldsymbol{\omega}}(t)$, and $\boldsymbol{\delta\omega}(t) = \boldsymbol{\omega}(t) - \hat{\boldsymbol{\omega}}(t)$ is the difference between the true and the estimated angular velocity. Assuming a constant angular velocity over the time interval Δt, it is possible to discretize the equation, which becomes:

$$\boldsymbol{\delta\alpha}_k = \boldsymbol{\delta\alpha}_{k-1} + [-\hat{\boldsymbol{\omega}}_k \Delta t]^{\times}\,\boldsymbol{\delta\alpha}_{k-1} + \boldsymbol{\delta\omega}_k \Delta t. \tag{85}$$

Similarly to the planar rotation case, the averaged angular velocity $\boldsymbol{\omega}_k^{(*)}$ is used to propagate the attitude. Therefore, the estimated angular velocity is

$$\hat{\boldsymbol{\omega}}_k = \widetilde{\boldsymbol{\omega}}_k^{(*)} - \hat{\boldsymbol{b}}_k^{(*)}, \tag{86}$$

and, by considering the measurement model described in eq. (70), the difference between the true and estimated angular velocity is therefore

$$\boldsymbol{\delta\omega}_k = \hat{\boldsymbol{b}}_k^{(*)} - \boldsymbol{b}_k^{(*)} - \boldsymbol{\nu}^{(*)}, \tag{87}$$

where $\boldsymbol{\nu}^{(*)} \sim \mathcal{N}\left(\mathbf{0}, \dfrac{\rho}{1+\rho}\sigma^2 \boldsymbol{I}_{3\times 3}\right)$. Considering the dynamics of the bias $\boldsymbol{b}_k^{(*)}$ described by eq. (91), the complete evolution of the attitude error vector is:

$$\boldsymbol{\delta\alpha}_k = \boldsymbol{\delta\alpha}_{k-1} - \left[\left(\widetilde{\boldsymbol{\omega}}_k^{(*)} - \hat{\boldsymbol{b}}_{k-1}^{(*)}\right)\Delta t\right]^{\times}\boldsymbol{\delta\alpha}_{k-1} + \left(\hat{\boldsymbol{b}}_{k-1}^{(*)} - \boldsymbol{b}_{k-1}^{(*)} - \boldsymbol{\nu}_k^{(*)} + \boldsymbol{\nu}_k^{(*),b}\right)\Delta t, \tag{88}$$

By linearizing the dynamic described by eq. (88), it is possible to propagate the covariance matrix from time $k-1$ to time k using eq. (35), in which

$$\begin{aligned}
\boldsymbol{\Phi} &= \begin{bmatrix} \boldsymbol{I}_{3\times 3} - \left[\left(\widetilde{\boldsymbol{\omega}}_k^{(*)} - \hat{\boldsymbol{b}}_{k-1}^{(*)}\right)\Delta t\right]^{\times} & -\Delta t \boldsymbol{I}_{3\times 3} & \mathbf{0}_{3\times 3} \\ \mathbf{0}_{3\times 3} & \boldsymbol{I}_{3\times 3} & \mathbf{0}_{3\times 3} \\ \mathbf{0}_{3\times 3} & \mathbf{0}_{3\times 3} & \boldsymbol{I}_{3\times 3} \end{bmatrix}, \\
\boldsymbol{B} &= \begin{bmatrix} \Delta t \boldsymbol{I}_{3\times 3} \\ \mathbf{0}_{6\times 3} \end{bmatrix}, \quad \boldsymbol{\Gamma} = \begin{bmatrix} -\Delta t \boldsymbol{I}_{3\times 3} & \mathbf{0}_{3\times 3} \\ \boldsymbol{I}_{3\times 3} & \mathbf{0}_{3\times 3} \\ \mathbf{0}_{3\times 3} & \boldsymbol{I}_{3\times 3} \end{bmatrix}, \\
\boldsymbol{U}_{k-1} = \frac{\rho}{1+\rho}\sigma^2 \boldsymbol{I}_{3\times 3}, &\quad \boldsymbol{Q}_{k-1} = \begin{bmatrix} \dfrac{\rho}{1+\rho}\sigma_b^2 \boldsymbol{I}_{3\times 3} & \mathbf{0}_{3\times 3} \\ \mathbf{0}_{3\times 3} & (1+\rho)\,\sigma_b^2 \boldsymbol{I}_{3\times 3} \end{bmatrix}.
\end{aligned} \tag{89}$$

During the time update the reference quaternion is propagated according to the dynamics:

$$\bar{\boldsymbol{q}}_k = \begin{bmatrix} \frac{1}{2}\hat{\boldsymbol{\omega}}_k \Delta t \\ 1 \end{bmatrix} \otimes \hat{\boldsymbol{q}}_{k-1} = \begin{bmatrix} \frac{1}{2}\left(\widetilde{\boldsymbol{\omega}}_k^{(*)} - \hat{\boldsymbol{b}}_k^{(*)}\right) \Delta t \\ 1 \end{bmatrix} \otimes \hat{\boldsymbol{q}}_{k-1}. \tag{90}$$

Regarding the propagation of the biases, taking the expectation of eqs. (81) and (82) leads to:

$$\bar{\boldsymbol{b}}_k^{(*)} = \hat{\boldsymbol{b}}_{k-1}^{(*)}, \tag{91}$$

$$\Delta\bar{\boldsymbol{b}}_k = \Delta\hat{\boldsymbol{b}}_{k-1}. \tag{92}$$

4.2.2 Measurement Update

After the propagation step, the state is updated using the difference in the angular velocity measurements. In the same fashion as eqs. (57) to (60), it can be proved that

$$\Delta\widetilde{\boldsymbol{\omega}}_k = \Delta\boldsymbol{b}_k + \boldsymbol{\nu}_k^{\Delta} \tag{93}$$

where $\boldsymbol{\nu}_k^{\Delta} \sim \mathcal{N}\left(\boldsymbol{0}, (1+\rho)\,\sigma^2 \boldsymbol{I}_{3\times3}\right)$. Therefore, it is possible to perform a classical Kalman update, described by eqs. (63) to (65), without linearization and without the need to consider the state at time $k-1$. In this case, the sensitivity matrix H is

$$\boldsymbol{H} = \begin{bmatrix} \boldsymbol{0}_{3\times3} & \boldsymbol{0}_{3\times3} & \boldsymbol{I}_{3\times3} \end{bmatrix}, \tag{94}$$

and the measurement covariance matrix $\boldsymbol{R}$ is

$$\boldsymbol{R} = (1+\rho)\,\sigma^2 \boldsymbol{I}_{3\times3}. \tag{95}$$

4.2.3 Star Tracker Update

In appendix B, we show that for a planar rotation, in the absence of an attitude measurement, only the bias difference is observable. The same consideration motivates the inclusion of an attitude measurement in the three-dimensional rotation case. Specifically, a star tracker measurement is introduced to ensure full system observability under persistence of excitation conditions.

A star tracker sensor measures the direction $\boldsymbol{c}_j$ of the j-*th* star in the body-fixed frame. Assuming the sensor can correctly recognize and match each star, the direction of the j-*th* star in the inertial frame is known. The approximate measurement model is therefore given by [3]:

$$\boldsymbol{c}_j = \boldsymbol{A}(\boldsymbol{q})\boldsymbol{r}_j + \boldsymbol{\nu}_j \tag{96}$$

where $\boldsymbol{\nu}_j \sim \mathcal{N}\left(\boldsymbol{0}, \sigma_j^2 \boldsymbol{I}_{3\times3}\right)$, $\boldsymbol{r}_j$ is the direction of the j-*th* star in the inertial frame, and $\boldsymbol{A}(\boldsymbol{q})$ is the direction cosine matrix that transforms vector coordinates from the inertial frame to the body frame. Considering measurements from n stars at time k,

the following holds:

$$\boldsymbol{y}_k = \begin{bmatrix} \boldsymbol{c}_1 \\ \boldsymbol{c}_2 \\ \vdots \\ \boldsymbol{c}_n \end{bmatrix} = \begin{bmatrix} \boldsymbol{A}(\boldsymbol{q}_k)\boldsymbol{r}_1 \\ \boldsymbol{A}(\boldsymbol{q}_k)\boldsymbol{r}_2 \\ \vdots \\ \boldsymbol{A}(\boldsymbol{q}_k)\boldsymbol{r}_n \end{bmatrix} + \begin{bmatrix} \boldsymbol{\nu}_1 \\ \boldsymbol{\nu}_2 \\ \vdots \\ \boldsymbol{\nu}_n \end{bmatrix} = \boldsymbol{h}(\boldsymbol{x}_k) + \boldsymbol{\nu}_k. \tag{97}$$

The true attitude matrix, $\boldsymbol{A}(\boldsymbol{q}_k)$, can be considered as the composition of the estimated attitude matrix, $\boldsymbol{A}(\hat{\boldsymbol{q}}_k)$, and the error direction cosine matrix, $\boldsymbol{A}(\boldsymbol{\delta q}_k)$:

$$\boldsymbol{A}(\boldsymbol{q}_k) = \boldsymbol{A}(\boldsymbol{\delta q}_k)\boldsymbol{A}(\hat{\boldsymbol{q}}_k). \tag{98}$$

Considering a first-order approximation of the error-attitude matrix, $\boldsymbol{A}(\boldsymbol{\delta q}_k)$ is given by:

$$\boldsymbol{A}(\boldsymbol{\delta q}_k) \approx \boldsymbol{I}_{3\times 3} - [\boldsymbol{\delta\alpha}_k]^{\times} \tag{99}$$

where $[\boldsymbol{\delta\alpha}_k]^{\times}$ is the skew-symmetric matrix associated with the small error vector $\boldsymbol{\delta\alpha}_k$. After linearization, the measurement model can be written as:

$$\boldsymbol{y}_k = \boldsymbol{H}_k\boldsymbol{x}_k + \boldsymbol{\nu}_k, \tag{100}$$

where:

$$\boldsymbol{H}_k = \begin{bmatrix} [\boldsymbol{A}(\boldsymbol{q}_k)\boldsymbol{r}_1]^{\times} & \boldsymbol{0}_{3\times 6} \\ [\boldsymbol{A}(\boldsymbol{q}_k)\boldsymbol{r}_2]^{\times} & \boldsymbol{0}_{3\times 6} \\ \vdots & \vdots \\ [\boldsymbol{A}(\boldsymbol{q}_k)\boldsymbol{r}_n]^{\times} & \boldsymbol{0}_{3\times 6} \end{bmatrix}. \tag{101}$$

4.3 Results and Discussion

The proposed method is compared with the approach by Marcus et al. [10], which employs distinct gyros for the propagation and measurement-update steps. In section 3, it was shown that, for planar rotations, propagating the state using one gyro measurement and updating with another yields the same estimate as propagating with the average angular rate and updating with the difference. However, due to the non-linear nature of three-dimensional attitude dynamics and the associated linearization, a similar analytical equivalence cannot be established for general spatial rotations. Therefore, to evaluate the performance of the two filtering strategies, a Monte Carlo simulation with 1,000 runs is performed.

The two methods are compared against each other and against the typical approach, which consists on utilizing a single gyro. This section is organized as follows: first, the Monte Carlo simulation setup is described, including sensor specifications and the procedure for generating the truth trajectory; then, the results are presented and discussed.

4.3.1 Monte Carlo Settings

The truth trajectory is generated by numerically integrating the continuous-time quaternion dynamics alongside the Euler equations [3]. The coupling dynamics are described by

$$\dot{\boldsymbol{q}}(t) = \frac{1}{2}\begin{bmatrix}\boldsymbol{\omega}(t)\\ 0\end{bmatrix} \otimes \boldsymbol{q}(t), \tag{102}$$

$$\dot{\boldsymbol{\omega}}(t) = -J^{-1}\left[\boldsymbol{\omega}(t) \times J\boldsymbol{\omega}(t)\right]. \tag{103}$$

The initial conditions and the inertia matrix are provided in table 1.

Table 1 Initial conditions of numerical integration.

Parameter	Unit	Value
$\boldsymbol{q}(0)$	-	$\begin{bmatrix}0 & 0 & 0 & 1\end{bmatrix}^T$
$\boldsymbol{\omega}(0)$	deg/s	$\begin{bmatrix}0.1 & 0.1 & 0\end{bmatrix}^T$
$\boldsymbol{J}$	kg m^2	$\begin{bmatrix}1 & 0 & 0\\ 0 & 2.5 & 0\\ 0 & 0 & 2\end{bmatrix}$

The numerical integration outputs are sampled at a fixed interval Δt_G, corresponding to the sampling rate of the gyros. The angular velocity measurements are then corrupted with a random noise sequence to simulate realistic gyro readings. Both gyros are assumed to have identical noise characteristics, i.e., $\rho = 1$. Regarding the evolution of the gyro biases, although their true dynamics evolve continuously, the following discrete-time approximation is applied for the truth simulation.

$$\boldsymbol{b}_k^{(i)} = \boldsymbol{b}_{k-1}^{(i)} + \boldsymbol{\nu}_b, \tag{104}$$

where $\boldsymbol{\nu}_b \sim \mathcal{N}(\boldsymbol{0}, \sigma_b^2 \boldsymbol{I}_{3\times 3})$. The noise characteristics of the gyros are summarized in table 2.

Table 2 Gyro's parameters.

Parameter	Unit	Value
Δt_G	s	0.01
ARW [9]	deg/h/$\sqrt{Hz}$	0.72
σ_b [9]	deg/h	0.05

Star tracker measurements are simulated by considering three orthonormal inertial reference directions,

$$\boldsymbol{r}_1 = \begin{bmatrix} 1 \\ 0 \\ 0 \end{bmatrix}, \quad \boldsymbol{r}_2 = \begin{bmatrix} 0 \\ 1 \\ 0 \end{bmatrix}, \quad \boldsymbol{r}_3 = \begin{bmatrix} 0 \\ 0 \\ 1 \end{bmatrix}, \tag{105}$$

projecting them in the body frame, and corrupting these measurements with random noise. The characteristics of the star tracker are provided in table 3.

Table 3 Star Tracker parameters.

Parameter	Unit	Value
Δt_{ST}	s	3
σ_{ST}	deg	0.01

Finally, the filters are initialized with the same initial state estimate for each Monte Carlo run, using the covariance matrix given in table 4.

Table 4 Initial covariance matrix.

Parameter	Unit	Value
$\boldsymbol{P}_{\alpha\alpha}$	deg^2	$0.1^2\boldsymbol{I}_{3\times3}$
$\boldsymbol{P}_{bb}$	deg^2/s^2	$0.01^2\boldsymbol{I}_{3\times3}$

4.3.2 Monte Carlo Results

The estimation errors obtained from the Monte Carlo analysis are shown in fig. 1 for the MEKF proposed by Marcus et al. [10] and in fig. 2 for the MEKF proposed in this work. These plots reveal that both methods are consistent, as the error mean remains zero and the true and filter covariances align perfectly. Furthermore, no significant difference is observed between the two plots. Both proposed approaches maintain bias observability.

To evaluate the accuracy of the proposed method, the steady-state root mean square error (RMSE) [18] is computed as

$$\text{RMSE} = \frac{1}{(N_\text{t} - N_\text{ss} + 1)N_\text{m}} \sum_{k=N_\text{ss}}^{N_\text{t}} \sum_{j=1}^{N_\text{m}} \sqrt{\sum_{i=1}^{N_\text{s}} \frac{(x_{k,j}^{(i)} - \hat{x}_{k,j}^{(i)})^2}{N_\text{s}}}, \tag{106}$$

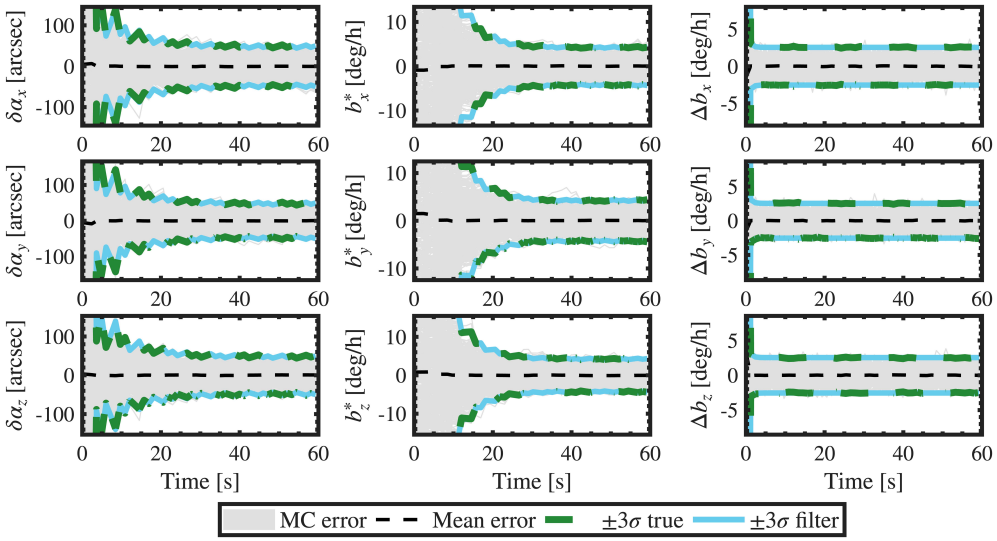


Fig. 1 Estimation error as a function of time using the MEKF proposed by Marcus et al. [10].

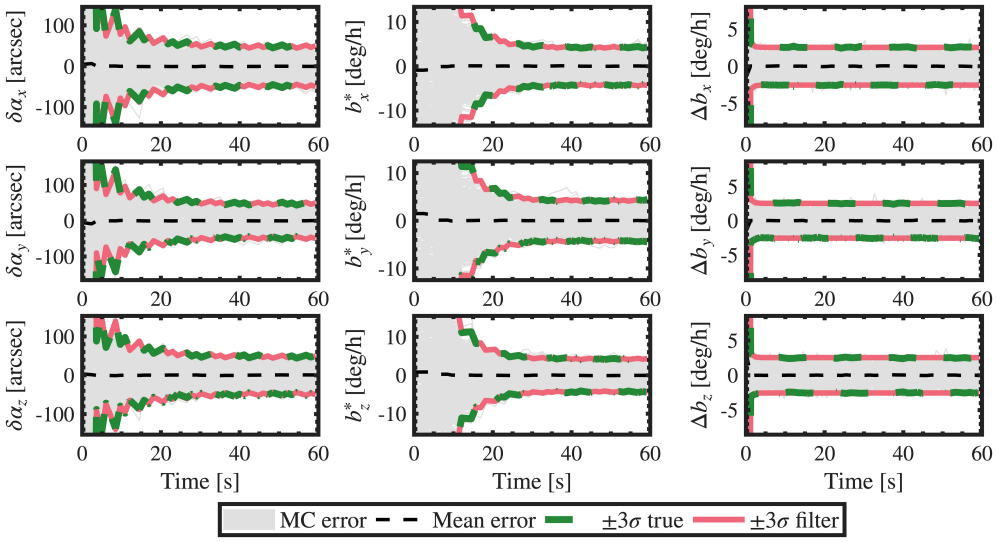


Fig. 2 Estimation error as a function of time using the MEKF proposed in this work.

where N_{ss} is chosen appropriately to ensure only the steady-state portion of the estimation results is considered, N_{t} is the total number of time steps, N_{m} is the number of Monte Carlo simulations, and N_{s} is the number of states. The results are summarized in table 5, which confirms that both methods are once again equivalent. Additionally, these results are compared to the conventional filtering approach, where only a

single gyro is used for estimation. The findings indicate that utilizing all available gyros improves attitude estimation accuracy by approximately 8% and bias estimation accuracy by approximately 22%.

Table 5 Time-averaged steady-state Root Mean Squared Error for the two methods analyzed and comparison with current state-of-the-art.

State	Averaging	Delayed Update	Single Gyro
$\boldsymbol{\delta\alpha}$ [arcsec]	14.861	14.861	16.119
$\boldsymbol{b}^{(1)}$ [deg/h]	1.3646	1.3646	1.6941
$\boldsymbol{b}^{(2)}$ [deg/h]	1.3652	1.3652	-

Finally, fig. 3 presents the results obtained by propagating the attitude using the average angular velocity measurement and updating it solely with the star tracker, without incorporating the update based on the differences in angular velocity. A comparison with figs. 1 and 2 clearly shows that the attitude and average bias estimates are identical. However, in this configuration, the difference between individual gyro biases is not observable. This outcome supports one of the central claims of this paper: the estimation of the bias differences is decoupled from the other state components and can be performed when accurate knowledge of individual biases is required, such as for FDI purposes.

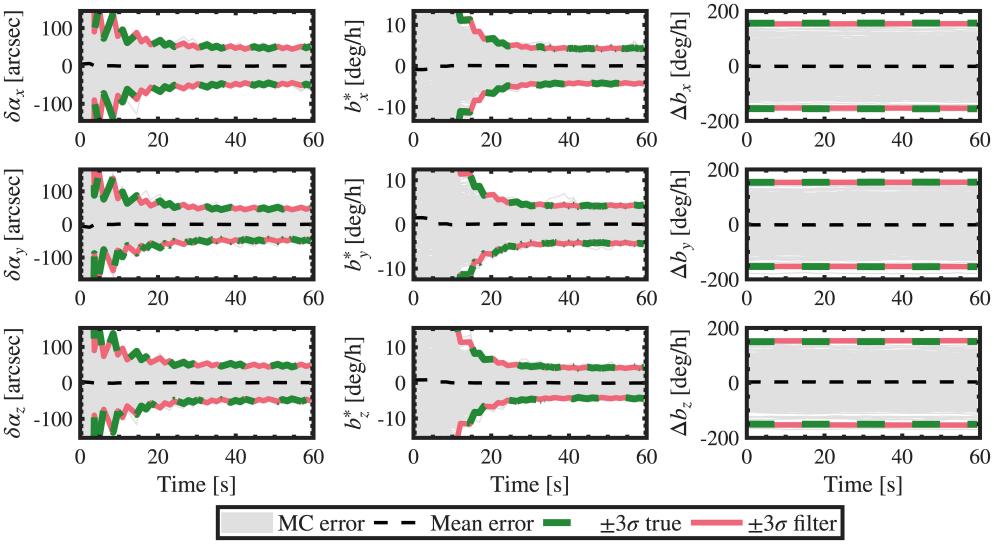


Fig. 3 Estimation error as a function of time for the results obtained averaging the gyro measurements without updating Δb.

5 Conclusions

This work proposes a novel method for fusing angular velocity measurements from all available gyros in redundant IMUs that provide fault-free estimates. For planar rotations, the proposed approach has been shown to be analytically equivalent to the strategy of using distinct gyros for the state propagation and measurement-update steps, as detailed in section 3. In the general three-axis case, however, an analytical equivalence proof is not feasible due to the necessary linearization of the nonlinear attitude dynamics and measurement models.

Monte Carlo simulations demonstrate that the two methods yield statistically equivalent performance in terms of estimation accuracy and filter consistency. Both approaches preserve full observability of the state, which is essential for enabling robust FDI capabilities, although FDI implementation is beyond the scope of this study. Notably, the proposed method avoids reliance on delayed-state Kalman filter updates, offering a more direct and computationally efficient fusion strategy.

The primary limitation of the proposed method is its assumption that all gyros have similar noise characteristics. In practice, this is rarely a significant concern, as redundant IMUs are typically composed of sensors with identical specifications. While the present analysis considers only two IMUs, the algorithm is readily extensible to larger numbers of gyros, enabling broader applicability in highly redundant systems.

Declarations

Ethical Approval and Consent to Participate

Not applicable.

Human Ethics

Not applicable.

Consent for Publication

Not applicable.

Availability of Supporting Data

The datasets generated and analyzed during the current study are available from the corresponding author upon reasonable request.

Competing Interests

The authors declare that they have no competing interests.

Funding

This material is based on research sponsored by the Air Force Office of Scientific Research (AFOSR) under agreement number FA9550-23-1-0646, *Create the Future Independent Research Effort (CFIRE).*

Authors' Contributions

A.R. implemented the code and wrote the main manuscript. R.Z. supervised and directed the research. All authors reviewed the manuscript.

Acknowledgements

Not applicable.

Clinical Trial Registration and Number

Not applicable.

Appendix A Angular Velocity Model Integration and Dual Updates

In many aerospace applications, angular velocity can be predicted by integrating a dynamical model. For spacecraft, this model is governed by the Euler equations [3]. For rovers, angular velocity can be determined from odometry measurements. Assume we have a model that provides an unbiased estimate $\hat{\omega}_k$ of the angular rate:

$$\hat{\omega}_k = \omega_k + \nu_m, \tag{A1}$$

$$\nu_m \sim \mathcal{N}\left(0,\, \sigma_m^2\right). \tag{A2}$$

In this case, we can use the angular velocity coming from the model $\hat{\omega}_k$ to propagate the state and the angular rates from the gyros $\widetilde{\omega}_k^{(1)}$, $\widetilde{\omega}_k^{(2)}$ to update the state. This method creates a framework in which dealing with correlated gyros is straightforward. The result of the propagation is $\theta_k \sim \mathcal{N}(\bar{\theta}_k, \bar{P}_k)$ where:

$$\bar{\theta}_k = \hat{\theta}_{k-1} + \hat{\omega}_k \Delta t, \tag{A3}$$

$$\bar{P}_k = P_{k-1} + \Delta t^2 \sigma_m^2. \tag{A4}$$

This estimate can be updated using data from gyro 1 and gyro 2, along with the delayed-state Kalman update applied earlier. In this case

$$\boldsymbol{H} = \begin{bmatrix} \frac{1}{\Delta t} \\ \frac{1}{\Delta t} \end{bmatrix}, \quad \boldsymbol{J} = \begin{bmatrix} -\frac{1}{\Delta t} \\ -\frac{1}{\Delta t} \end{bmatrix}, \quad \boldsymbol{R} = \begin{bmatrix} \sigma_{(1)}^2 & 0 \\ 0 & \sigma_{(2)}^2 \end{bmatrix}. \tag{A5}$$

It follows that

$$\boldsymbol{K}_k = \Delta t \begin{bmatrix} \dfrac{\sigma_{(2)}^2 \sigma_m^2}{\sigma_{(1)}^2\sigma_{(2)}^2 + \sigma_{(1)}^2\sigma_m^2 + \sigma_{(2)}^2\sigma_m^2} & \dfrac{\sigma_{(1)}^2 \sigma_m^2}{\sigma_{(1)}^2\sigma_{(2)}^2 + \sigma_{(1)}^2\sigma_m^2 + \sigma_{(2)}^2\sigma_m^2} \end{bmatrix}, \tag{A6}$$

$$\boldsymbol{L}_k = \begin{bmatrix} \sigma_{(1)}^2 + \sigma_m^2 & \sigma_m^2 \\ \sigma_m^2 & \sigma_{(2)}^2 + \sigma_m^2 \end{bmatrix}. \tag{A7}$$

After the update step, the optimal estimate at time k, given a model for the angular velocity $\hat{\omega}_k$, and uncorrelated measurements from distinct gyros $\widetilde{\omega}_k^{(1)}$, $\widetilde{\omega}_k^{(2)}$, is

$$\hat{\theta}_k = \hat{\theta}_{k-1} + \Delta t \frac{\sigma_{(1)}^2 \sigma_{(2)}^2 \hat{\omega}_k + \sigma_{(2)}^2 \sigma_m^2 \widetilde{\omega}_k^{(1)} + \sigma_{(1)}^2 \sigma_m^2 \widetilde{\omega}_k^{(2)}}{\sigma_{(1)}^2 \sigma_{(2)}^2 + \sigma_{(1)}^2 \sigma_m^2 + \sigma_{(2)}^2 \sigma_m^2}, \tag{A8}$$

$$P_k = P_{k-1} + \Delta t^2 \frac{\sigma_{(1)}^2 \sigma_{(2)}^2 \sigma_m^2}{\sigma_{(1)}^2 \sigma_{(2)}^2 + \sigma_{(1)}^2 \sigma_m^2 + \sigma_{(2)}^2 \sigma_m^2}. \tag{A9}$$

If the angular velocity model is unknown, i.e. $\sigma_m^2 \to \infty$, the estimated angle θ is the same as the one obtained only by propagating with an average angular rate.

$$\lim_{\sigma_m^2 \to \infty} \hat{\theta}_k = \hat{\theta}_{k-1} + \Delta t \frac{\sigma_{(2)}^2 \widetilde{\omega}_k^{(1)} + \sigma_{(1)}^2 \widetilde{\omega}_k^{(2)}}{\sigma_{(1)}^2 + \sigma_{(2)}^2}, \tag{A10}$$

$$\lim_{\sigma_m^2 \to \infty} \hat{P}_k = \hat{P}_{k-1} + \Delta t^2 \frac{\sigma_{(1)}^2 \sigma_{(2)}^2}{\sigma_{(1)}^2 + \sigma_{(2)}^2}. \tag{A11}$$

Following this framework, an optimal estimate can be found if the gyros are correlated. The modeled angular velocity can be used to propagate the attitude, while the measurements $\widetilde{\omega}_k^{(1)}$, $\widetilde{\omega}_k^{(2)}$ to update the estimate. In this case, the measurement covariance matrix is

$$\boldsymbol{R} = \begin{bmatrix} \sigma_{(1)}^2 & \sigma_{(1,2)}^2 \\ \sigma_{(1,2)}^2 & \sigma_{(2)}^2 \end{bmatrix}. \tag{A12}$$

If the modeled angular velocity is unknown, i.e. $\sigma_m^2 \to \infty$, the optimal estimate in the case in which the gyros are correlated and no other information is available is

$$\hat{\theta}_k = \hat{\theta}_{k-1} + \Delta t \frac{\left(\sigma_{(2)}^2 - \sigma_{(1,2)}^2\right) \widetilde{\omega}_k^{(1)} + \left(\sigma_{(1)}^2 - \sigma_{(1,2)}^2\right) \widetilde{\omega}_k^{(2)}}{\sigma_{(1)}^2 + \sigma_{(2)}^2 - 2\sigma_{(1,2)}^2}, \tag{A13}$$

$$P_k = P_{k-1} + \Delta t^2 \frac{\sigma_{(1)}^2 \sigma_{(2)}^2 - \sigma_{(1,2)}^4}{\sigma_{(1)}^2 + \sigma_{(2)}^2 - 2\sigma_{(1,2)}^2}. \tag{A14}$$

Lemma 1 (Optimal Averaging of Correlated Gyros)**.** *Consider two angular velocity measurements $\widetilde{\omega}_k^{(1)}$ and $\widetilde{\omega}_k^{(2)}$, which may be correlated such that $\mathbb{E}[\nu_k^{(1)} \nu_k^{(2)}] = \sigma_{(1,2)}^2$. The MMSE estimate of the attitude, obtained by linearly combining these measurements, is given by*

$$\hat{\theta}_k = \hat{\theta}_{k-1} + \Delta t \, \frac{\left(\sigma_{(2)}^2 - \sigma_{(1,2)}^2\right) \widetilde{\omega}_k^{(1)} + \left(\sigma_{(1)}^2 - \sigma_{(1,2)}^2\right) \widetilde{\omega}_k^{(2)}}{\sigma_{(1)}^2 + \sigma_{(2)}^2 - 2\sigma_{(1,2)}^2}, \tag{A15}$$

$$P_k = P_{k-1} + \Delta t^2 \, \frac{\sigma_{(1)}^2 \sigma_{(2)}^2 - \sigma_{(1,2)}^4}{\sigma_{(1)}^2 + \sigma_{(2)}^2 - 2\sigma_{(1,2)}^2}. \tag{A16}$$

Proof Assume the attitude is propagated as

$$\hat{\theta}_k = \hat{\theta}_{k-1} + \Delta t \left(\alpha\, \widetilde{\omega}_k^{(1)} + \beta\, \widetilde{\omega}_k^{(2)} \right). \tag{A17}$$

Under the assumptions of finite means and variances, the MMSE estimator is unbiased. Therefore:

$$\mathbb{E}\left[\hat{\theta}_k - \theta_k\right] = \mathbb{E}\left[\hat{\theta}_{k-1} + \Delta t \left(\alpha\widetilde{\omega}_k^{(1)} + \beta\widetilde{\omega}_k^{(2)}\right) - \theta_{k-1} - \Delta t\omega_k\right] \tag{A18}$$

$$= \Delta t\, \omega_k \left(\alpha + \beta - 1\right). \tag{A19}$$

Therefore, the unbiasedness condition requires $\alpha + \beta = 1$, yielding

$$\hat{\theta}_k = \hat{\theta}_{k-1} + \Delta t \left(\widetilde{\omega}_k^{(1)} + \beta \left(\widetilde{\omega}_k^{(2)} - \widetilde{\omega}_k^{(1)} \right) \right). \tag{A20}$$

The second condition for optimality is that the estimation covariance is minimized:

$$P_k = P_{k-1} + \Delta t^2 \left[\sigma_{(1)}^2 + \beta^2(\sigma_{(1)}^2 + \sigma_{(2)}^2) - 2\beta\sigma_{(1)}^2 + 2\beta(1-\beta)\sigma_{(1,2)}^2 \right]. \tag{A21}$$

Setting $\partial P_k / \partial \beta = 0$ yields

$$\beta = \frac{\sigma_{(1)}^2 - \sigma_{(1,2)}^2}{\sigma_{(1)}^2 + \sigma_{(2)}^2 - 2\sigma_{(1,2)}^2}. \tag{A22}$$

Substituting this value of β into the estimator expression leads directly to eqs. (A15) and (A16), which proves the lemma. □

For a general case, in which measurements from N gyros are available, and the measurement can be correlated, we can get the optimal estimate by averaging the angular rates

$$\boldsymbol{R} = \begin{bmatrix} \sigma_{(1)}^2 & \sigma_{(1,2)}^2 & \cdots & \sigma_{(1,N)}^2 \\ \sigma_{(1,2)}^2 & \sigma_{(2)}^2 & \cdots & \sigma_{(2,N)}^2 \\ \vdots & \vdots & \ddots & \vdots \\ \sigma_{(1,N)}^2 & \sigma_{(2,N)}^2 & \cdots & \sigma_{(N)}^2 \end{bmatrix}, \quad \boldsymbol{\Gamma} = \boldsymbol{R}^{-1}, \tag{A23}$$

$$\boldsymbol{\Gamma} = \begin{bmatrix} \gamma_{(1)}^2 & \gamma_{(1,2)}^2 & \cdots & \gamma_{(1,N)}^2 \\ \gamma_{(1,2)}^2 & \gamma_{(2)}^2 & \cdots & \gamma_{(2,N)}^2 \\ \vdots & \vdots & \ddots & \vdots \\ \gamma_{(1,N)}^2 & \gamma_{(2,N)}^2 & \cdots & \gamma_{(N)}^2 \end{bmatrix} \tag{A24}$$

$$\widetilde{\omega}_k^{(*)} = \frac{\sum_{i=1}^N \sum_{j=1}^N \gamma_{ij}\, \widetilde{\omega}_k^{(i)}}{\sum_{i=1}^N \sum_{j=1}^N \gamma_{ij}}, \tag{A25}$$

$$\sigma_{(*)}^2 = \frac{1}{\sum_{i=1}^N \sum_{j=1}^N \gamma_{ij}}, \tag{A26}$$

$$\widetilde{\omega}_k^{(*)} \sim \mathcal{N}\left(\omega_k, \sigma_{(*)}^2\right), \tag{A27}$$

and using this angular rate to propagate the estimate from time $k-1$ to time k.

Appendix B Observability Analysis and Attitude Measurement

Consider a generic linear time-invariant system in discrete time

$$\boldsymbol{x}_{k+1} = \boldsymbol{\Phi}\boldsymbol{x}_k + \boldsymbol{B}\boldsymbol{u}_k, \tag{B28}$$
$$\boldsymbol{z}_k = \boldsymbol{H}\boldsymbol{x}_k + \boldsymbol{D}\boldsymbol{u}_k. \tag{B29}$$

The observability matrix can be computed as:

$$\mathcal{O} = \begin{bmatrix} \boldsymbol{H} \\ \boldsymbol{H}\boldsymbol{\Phi} \\ \boldsymbol{H}\boldsymbol{\Phi}^2 \\ \vdots \\ \boldsymbol{H}\boldsymbol{\Phi}^{m-1} \end{bmatrix}, \tag{B30}$$

where m is the number of states.

In the method proposed in section 3.2, the $\boldsymbol{\Phi}$ and $\boldsymbol{H}$ matrices are defined respectively in eqs. (54) and (62). Therefore, the observability matrix becomes:

$$\mathcal{O} = \begin{bmatrix} \boldsymbol{H} \\ \boldsymbol{H}\boldsymbol{\Phi} \\ \boldsymbol{H}\boldsymbol{\Phi}^2 \end{bmatrix} = \begin{bmatrix} 0 & 0 & 1 \\ 0 & 0 & 1 \\ 0 & 0 & 1 \end{bmatrix}. \tag{B31}$$

It is evident that this matrix has rank 1, as only the difference in biases Δb is observable due to its uncorrelation with the other states $b^{(*)}$, θ.

To make the system fully observable, a measurement of the angle $\widetilde{\theta}_k$ is introduced. The measurement model in this case is:

$$\widetilde{\theta}_k = \theta_k + \nu_k^{\theta}, \tag{B32}$$

where $\nu_k^{\theta} \sim \mathcal{N}\left(0, \sigma_{\theta}^2\right)$.

It is clear that the state can be updated using both the angular measurement and the difference in angular velocity. The complete measurement model is:

$$\boldsymbol{z}_k = \begin{bmatrix} \tilde{\theta}_k \\ \Delta\tilde{\omega}_k \end{bmatrix} = \boldsymbol{H}\boldsymbol{x}_k + \boldsymbol{v}_k, \tag{B33}$$

where $\boldsymbol{v}_k \sim \mathcal{N}(\boldsymbol{0}, \boldsymbol{R})$ and

$$\boldsymbol{H} = \begin{bmatrix} 1 & 0 & 0 \\ 0 & 0 & 1 \end{bmatrix}, \quad \boldsymbol{R} = \begin{bmatrix} \sigma_{\theta}^2 & 0 \\ 0 & (1+\rho)\,\sigma^2 \end{bmatrix}. \tag{B34}$$

In this case, the observability matrix can be recomputed, yielding:

$$\mathcal{O} = \begin{bmatrix} \boldsymbol{H} \\ \boldsymbol{H\Phi} \\ \boldsymbol{H\Phi}^2 \end{bmatrix} = \begin{bmatrix} 1 & 0 & 0 \\ 0 & 0 & 1 \\ 1 & -\Delta t & 0 \\ 0 & 0 & 1 \\ 1 & -2\Delta t & 0 \\ 0 & 0 & 1 \end{bmatrix}. \tag{B35}$$

It is evident that, under the basic assumption of $\Delta t \neq 0$, the observability matrix is full rank, meaning all the states are observable.

References

[1] Mamich, H., D'Souza, C.: Orion preliminary navigation system design. In: AIAA Guidance, Navigation and Control Conference and Exhibit, p. 7295 (2008)

[2] Goodman, J.L.: Space shuttle navigation in the gps era. In: Proceedings of the 2001 National Technical Meeting of The Institute of Navigation, pp. 709–724 (2001)

[3] Markley, F.L., Crassidis, J.L.: Fundamentals of Spacecraft Attitude Determination and Control. Springer, New York, NY (2014). https://doi.org/10.1007/978-1-4939-0802-8

[4] Thibodeau, J., Bauer, S.R.: Redundancy management of the space shuttle inertial measurement units. In: Guidance and Control Conference, p. 1561 (1982)

[5] Gertler, J.: Fault Detection and Diagnosis in Engineering Systems, 2nd edn. CRC Press, Boca Raton, FL (2017)

[6] Alteriis, G., Conte, C., Moriello, R.S.L., Accardo, D.: Use of consumer-grade mems inertial sensors for accurate attitude determination of drones. In: 2020 IEEE 7th International Workshop on Metrology for AeroSpace (MetroAeroSpace), pp. 534–538 (2020). IEEE

[7] Fontanella, R., Alteriis, G., Accardo, D., Moriello, R.S.L., Angrisani, L.: Advanced low-cost integrated inertial systems with multiple consumer grade sensors. In: 2018 IEEE/AIAA 37th Digital Avionics Systems Conference (DASC), pp. 1–8 (2018). IEEE

[8] Patel, U.N., Faruque, I.A.: Multi-imu based alternate navigation frameworks: Performance & comparison for uas. IEEE Access **10**, 17565–17577 (2022)

[9] Beaudoin, Y., Desbiens, A., Gagnon, E., Landry Jr, R.: Satellite launcher navigation with one versus three imus: Sensor positioning and data fusion model analysis. Sensors **18**(6), 1872 (2018)

[10] Marcus, C.L., Zanetti, R., Getchius, J.W.: Attitude estimation and optimal relative orientation of redundant inertial measurement units. Journal of Guidance, Control, and Dynamics (2025). Accepted for pubblication

[11] Rigato, A., Zanetti, R.: Attitude estimation of planar rotations using redundant gyroscopes. In: AAS/AIAA Astrodynamics Specialist Conference, Boston, MA (2025)

[12] Butcher, J.C.: Numerical Methods for Ordinary Differential Equations, 3rd edn. John Wiley & Sons, Chichester, UK (2016)

[13] Kalman, R.E., *et al.*: A new approach to linear filtering and prediction problems [j]. Journal of basic Engineering **82**(1), 35–45 (1960)

[14] Maybeck, P.S.: Stochastic Models, Estimation, and Control vol. 1. Academic Press, New York, NY (1982)

[15] Brown, R.G., Hwang, P.Y.: Introduction to random signals and applied kalman filtering: with matlab exercises and solutions. Introduction to random signals and applied Kalman filtering: with MATLAB exercises and solutions (1997)

[16] Crassidis, J.L., Junkins, J.L.: Optimal Estimation of Dynamic Systems, 1st edn. Chapman & Hall/CRC, Boca Raton, FL (2004)

[17] Shuster, M.D.: The nature of the quaternion. The Journal of the Astronautical Sciences **56**(3), 359–373 (2008)

[18] Bar-Shalom, Y., Li, X.R., Kirubarajan, T.: Estimation with Applications to Tracking and Navigation: Theory, Algorithms, and Software, 1st edn. John Wiley & Sons, Hoboken, NJ (2004)